JCS ePress online publication date 11 January 2011

The pericentriolar satellite protein CEP90 is crucial for integrity of the mitotic spindle pole

Kyeongmi Kim and Kunsoo Rhee*

Department of Biological Sciences, Seoul National University, Seoul 151-747, Korea

*Author for correspondence (rheek@snu.ac.kr)

Accepted 27 September 2010
Journal of Cell Science 124, 338-347

doi:10.1242/jcs.078329

Summary

Pericentriolar satellites are electron-dense granules that are concentrated around the centrosome. They are involved in the recruitment of centrosomal proteins and microtubule organization in interphase cells, but their mitotic functions are largely unknown. In this study, we characterize CEP90 as a component of pericentriolar satellites. CEP90 is present both in the centrosome and in the cytoplasm, but is transiently concentrated at the centrosome once cells enter mitosis. Depletion of CEP90 caused mitotic arrest with misaligned chromosomes. Spindle pole fragmentation was the most characteristic phenotype in CEP90-depleted cells. Spindle poles were fragmented as soon as the spindles attached, suggesting that the mechanical forces of spindle microtubules physically stress the structure of CEP90-depleted spindle poles. Based on these results, we propose that CEP90 is crucial for maintaining the integrity of spindle poles during mitosis.

Key words: CEP90, Pericentriolar satellites, Spindle pole, Centrosome

Introduction

The centrosome in animal cells functions as a microtubule-organizing center (MTOC) to establish a cellular microtubule network that affects cellular morphology, movement and intracellular material transport. A cell that enters mitosis undergoes a dramatic structural change, which is accompanied by the centrosome maturation process. First, the interphase microtubules are rapidly degraded. At the same time, pericentriolar material (PCM) proteins, such as pericentrin and γ-tubulin, are actively recruited to the centrosome and, as a result, a massive increase in microtubule nucleation is observed at the centrosomes in early mitosis (Dictenberg et al., 1998; Khodjakov and Rieder, 1999; Piehl et al., 2004). Mitotic microtubules are also nucleated from other sites, such as chromosomes and spindle microtubules, but are soon integrated into preformed spindle microtubules and eventually linked to a common pole (Khodjakov et al., 2003; Maiato et al., 2004; Mahoney et al., 2006).

During mitosis, bipolar spindle formation is indispensable for accurate segregation of chromosomes. Depletion of centrosomal components often results in monopolar or multipolar spindles, suggesting that centrosome integrity is crucial for maintenance of spindle bipolarity (Garrett et al., 2002; Cassimeris and Morabito, 2004; Cho et al., 2006; Oshimori et al., 2006; Thein et al., 2007; Yang et al., 2008; Wu et al., 2008). In addition, motor proteins, such as HSET and dynein, contribute to the focusing of spindle microtubules into poles (Gaglio et al., 1997; Gordon et al., 2001). Non-motor proteins, such as NuMA, are also involved in spindle formation through their interactions with dynein (Merdes et al., 1996; Khodjakov et al., 2003; Silk et al., 2009). Additional protein components in the centrosome and spindle microtubules are probably required for bipolar spindle formation during mitosis.

Pericentriolar satellites are electron-dense granules that accumulate around centrosomes (Kubo et al., 1999; Kubo and Tsukita, 2003). The existence of pericentriolar satellites has been known for many years, but their composition, as well as their physiological functions, are not yet fully understood. Pericentriolar satellites are thought to be involved in transport of centrosomal proteins because knockdown of PCM-1 which is a major component of pericentriolar satellites, results in the reduction of several centrosomal proteins (Dammermann and Merdes, 2002; Hames et al., 2005). Depletion of PCM-1 also results in a reduction in microtubule-organizing activity, suggesting that pericentriolar satellites affect the microtubule-anchoring activity of the centrosome (Dammermann and Merdes, 2002). Characterization of the protein components of pericentriolar satellites should allow the elucidation of additional functions of these structures.

The human centrosome consists of hundreds of proteins, many of which have not yet been characterized. We characterized a centrosomal protein that had previously been identified as progesterone-induced-blocking factor 1 (PIBF1), a 34 kDa immunomodulatory protein that is secreted by activated lymphocytes during pregnancy (Szekeres-Bartho et al., 2001). We named this protein CEP90 based on its expected molecular weight. CEP90 is a larger isoform of PIBF1, consisting of the full c13orf24 open reading frame (Polgar et al., 2003). Proteomic analysis revealed that CEP90 is a core component of the human centrosome (Andersen et al., 2003). In this study, we show that CEP90 is a pericentriolar satellite protein that is crucial for integrity of the mitotic spindle pole.

Results

CEP90 localizes at the pericentriolar satellites

To investigate centrosome structure and function, we decided to characterize the centrosomal proteins that were identified in a proteomic analysis (Andersen et al., 2003). CEP90 is a centrosome protein whose subcellular localization was determined by an immunofluorescence staining study (Lachmann et al., 2004). We raised an antibody against the bacterially expressed GST–CEP90 fusion protein and affinity purified it. This antibody specifically recognized the endogenous CEP90 protein in an immunoblot

Journal of Cell Science

analysis (Fig. 1A). We also observed that the CEP90 antibody specifically immunostained the centrosome (Fig. 1B). However, the staining pattern of CEP90 was distinct from that of γ-tubulin, because the CEP90 aggregates were detected not only at the centrosome, but also in the surrounding area, and the signals were reduced at mitotic spindle poles (Fig. 1B). This staining pattern is similar to that of PCM-1, a component of the pericentriolar satellites (Kubo et al., 1999; Kubo and Tsukita, 2003). In fact, the coimmunostaining results revealed that CEP90 and PCM-1 were colocalized at the pericentriolar satellites in both interphase and mitotic cells (Fig. 1C). Furthermore, the coimmunoprecipitation assay revealed that CEP90 was physically associated with the pericentriolar satellite proteins PCM-1 and BBS4 (Bardet–Biedl syndrome 4) (Kim et al., 2004) (Fig. 1D). These results indicate that CEP90 is a component of pericentriolar satellites. The CEP90 signals disappeared from the pericentriolar satellites in PCM-1-depleted cells, leaving a small amount at the centrosomes in both interphase and mitotic cells (Fig. 1E,F). This result suggests that CEP90 localization at pericentriolar satellites is dependent on PCM-1 and that there exists a PCM-1-independent pool of CEP90 at the centrosome.

Centrosomal accumulation of CEP90 depends on microtubules and the dynein–dynactin complex

We observed the subcellular distribution of CEP90 in HeLa cells whose microtubule networks were disturbed with nocodazole. CEP90 aggregates were scattered throughout the cytoplasm of the nocodazole-treated cells (Fig. 2A). At the same time, a fraction of CEP90 was located at the centrosome in a microtubule-independent manner (Fig. 2A). We also observed scattered CEP90 signals in cells expressing GFP–dynamitin in which cellular dynein–dynactin activities were disrupted (Fig. 2B) (Echeverri et al., 1996). These

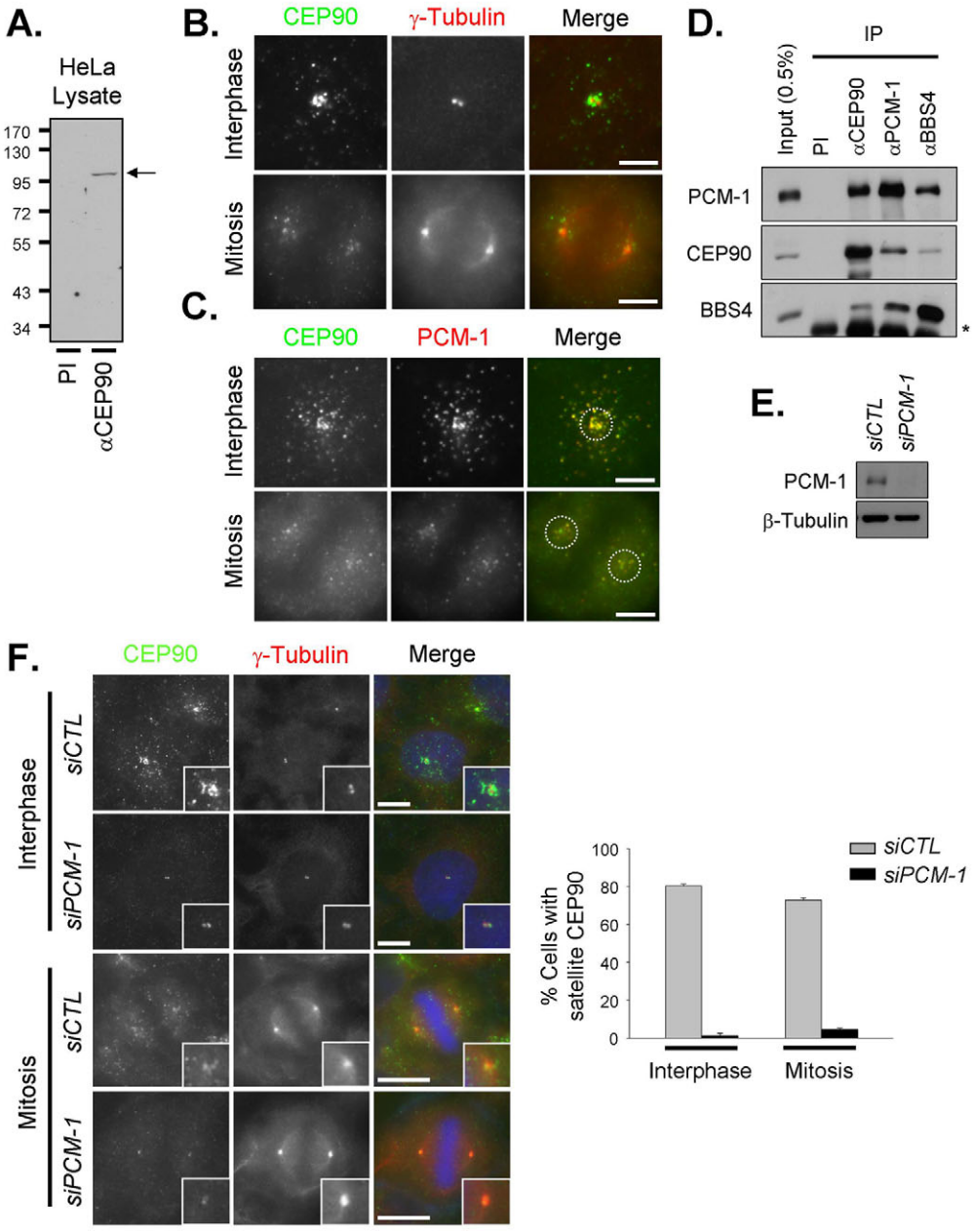

Fig. 1. CEP90 localization at pericentriolar satellites. (**A**) HeLa lysates subjected to immunoblot analysis with anti-CEP90 antibody or with preimmune serum (PI). (**B**) Centrosomes in HeLa cells at interphase and mitotic metaphase coimmunostained with antibodies specific to CEP90 (green) and γ-tubulin (red). Scale bars: 5 µm. (**C**) Centrosomes in HeLa cells at interphase and mitotic metaphase coimmunostained with antibodies specific to CEP90 (green) and PCM-1 (red). The centrosomal area is circled. Scale bars: 5 µm. (**D**) Asynchronous 293T lysates (L) were immunoprecipitated with preimmune serum (PI) or with anti-sera against CEP90, PCM-1 and BBS4 and subjected to immunoblot analysis with the same antibodies. *, IgG heavy chain. (**E**) HeLa cells were transfected with control (*siCTL*) or PCM-1 (*siPCM-1*) siRNAs. Forty-eight hours later, the lysates were subjected to immunoblot analysis with antibodies specific to PCM-1 and β-tubulin. (**F**) Control and PCM-1-depleted cells coimmunostained with antibodies specific to CEP90 (green) and γ-tubulin (red), along with DAPI (blue) staining. The number of cells with CEP90 at pericentriolar satellites was counted in the interphase and mitotic populations (graph on right). Over 200 cells were analyzed at each experimental group in two independent experiments. Insets are magnified views of the centrosomes. Scale bars: 10 µm.

results are consistent with previous reports in which the centrosomal accumulation of PCM-1 depends on microtubule network and dynein–dynactin activity (Dammermann and Merdes, 2002; Kubo and Tsukita, 2003).

A rapid and transient accumulation of CEP90 at the centrosome in early mitosis

Immunoblot analysis with a synchronized cell population revealed that the cellular protein levels of CEP90 were constant throughout the cell cycle (Fig. 3A). However, centrosomal CEP90 levels, as determined by immunostaining analysis, fluctuated in a cell-cycle-stage-specific manner. In interphase cells, CEP90 aggregates were distributed both in the centrosomal area and in the cytoplasm (Fig. 3B). Once cells entered mitosis, the CEP90 aggregates were concentrated at two separate centrosomes, leaving a small amount in the cytoplasm (Fig. 3B). The centrosomal CEP90 levels were reduced dramatically as soon as the cells entered metaphase and recovered again in telophase (Fig. 3B). A rapid and transient accumulation of CEP90 in early mitosis suggests its involvement in a specific function at this stage, such as spindle pole formation.

CEP90 knockdown results in abnormal spindles and chromosome misalignment

We knocked down *CEP90* expression by siRNA transfection. Immunoblot analysis revealed that the cellular CEP90 protein was reduced to an undetectable level 72 hours after *siCEP90* transfection (Fig. 4A). The centrosomal CEP90 signal was also undetectable, whereas the centrosomal γ-tubulin signal remained intact (Fig. 4B). In fact, the interphase centrosome looked intact in CEP90-depleted cells (Fig. 4B; see also Fig. 7A). We observed an increase in the mitotic cell population in CEP90-depleted cells, as determined by levels of cyclin B and phosphorylated histone H3 (Fig. 4A), and microscopic observations (Fig. 4C). The mitotic index in the CEP90-depleted population was four times higher than that of the control population (Fig. 4C). FACS analysis revealed that CEP90 depletion induced an increase in the G2–M phase population (21.5±2.0% versus 15.4±1.3% of the control group in three independent experiments), which is consistent with the microscopic observations (Fig. 4D). The relative proportions of prometaphase and metaphase cells increased in the CEP90-depleted mitotic population (Fig. 4E). These observations suggest that CEP90 is crucial for mitotic progression.

Mitotic defects in CEP90-depleted cells were examined carefully. First, we observed an increase in monopolar and multipolar spindles in the CEP90-depleted cell population (Fig. 5A). Second, even bipolar spindles in the CEP90-depleted cells did not look normal; they were elongated and sometimes asymmetrically curved (Fig. 5A). The distance between the spindle poles in CEP90-depleted cells was larger than that in control cells (Fig. 5B). Third, chromosome misalignment was present in about two thirds of the CEP90-depleted cells (Fig. 5C). A few chromosomes failed to congress and remained near a spindle pole even after an apparent metaphase plate was formed (Fig. 5C). Strong BubR1 and Mad2 signals were detected at the misaligned chromosomes in the CEP90-depleted cells (Fig. 5D,E). These results indicate that the spindle checkpoint was not satisfied owing to the presence of unattached or tensionless kinetochores in CEP90-depleted cells (Waters et al., 1998; Skoufias et al., 2001). Therefore, we conclude that the accumulation of mitotic cells caused by CEP90 depletion is due to abnormalities in spindle formation and defects in chromosome congression.

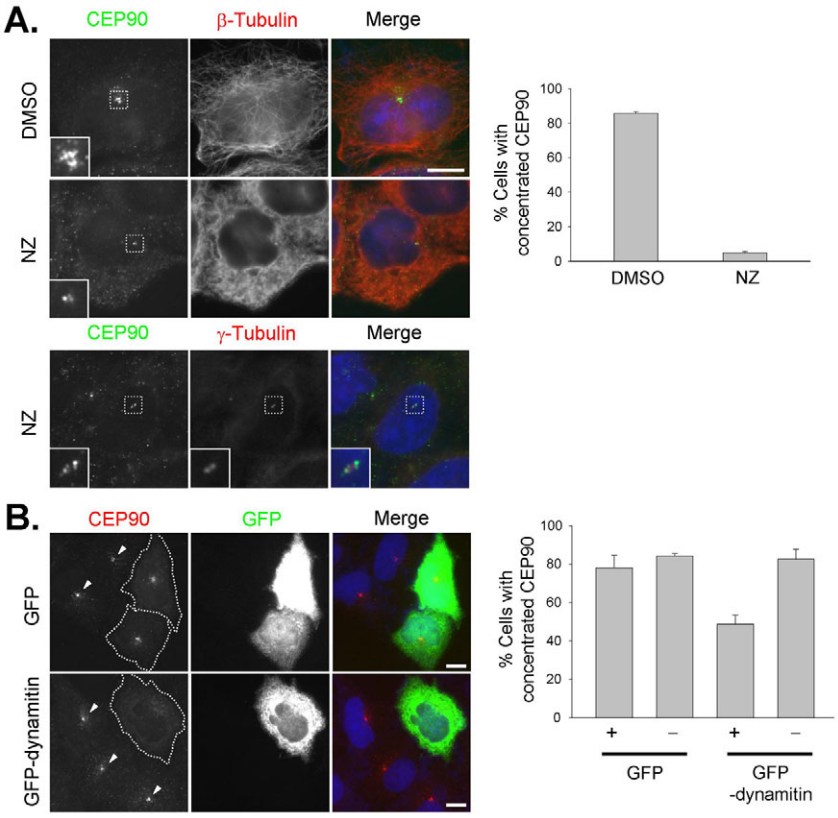

Fig. 2. Centrosomal accumulation of CEP90 depends on microtubules and the dynein–dynactin complex. (**A**) HeLa cells were treated with nocodazole (NZ) for 2 hours to disrupt the microtubule network. Control cells were treated with DMSO. CEP90 (green) was coimmunostained along with β-tubulin or γ-tubulin (red). Insets are magnified views of the centrosomes. The cells with centrosome-concentrated CEP90 were counted (right). Over 300 cells were analyzed in three independent experiments. (**B**) After transfection with GFP or GFP–dynamitin, HeLa cells were coimmunostained with antibodies against CEP90 (red) and GFP (green). Boundaries of the transfected cells are outlined. Arrowheads indicate the centrosomes in untransfected cells. The cells with centrosome-concentrated CEP90 were counted in both DNA-transfected (+) and untransfected cells (–) (graph on right). Over 200 cells were analyzed in two independent experiments. Scale bars: 10 μm.

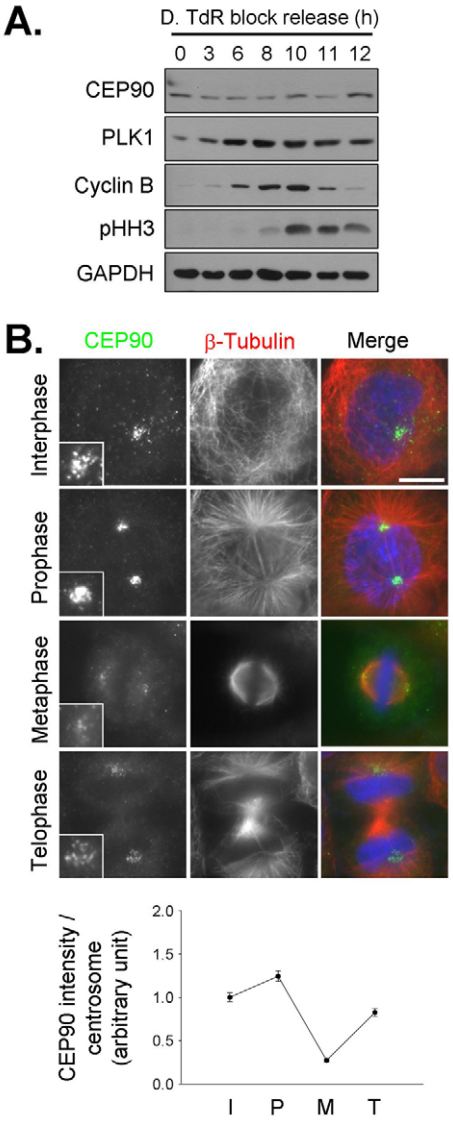

Fig. 3. Centrosomal CEP90 levels during the cell cycle. (**A**) The cell cycle of HeLa cells was arrested at G1–S phase with a double thymidine block and released synchronously. At the indicated time points, cells were harvested for immunoblot analysis with antibodies specific to CEP90, PLK1, cyclin B, phosphorylated histone H3 (pHH3) and GAPDH. (**B**) HeLa cells coimmunostained with antibodies against CEP90 (green) and β-tubulin (red). Insets are magnified views of the centrosomes. Interphase (I), prophase (P), metaphase (M) and telophase (T) cells were identified by spindle and chromosome morphology. The centrosomal CEP90 levels were determined by measuring the immunofluorescence intensity of CEP90 at the centrosome (bottom). Sixty centrosomes were measured per experimental group in three independent experiments. The results are presented as the mean ± s.e. Scale bar: 10 µm.

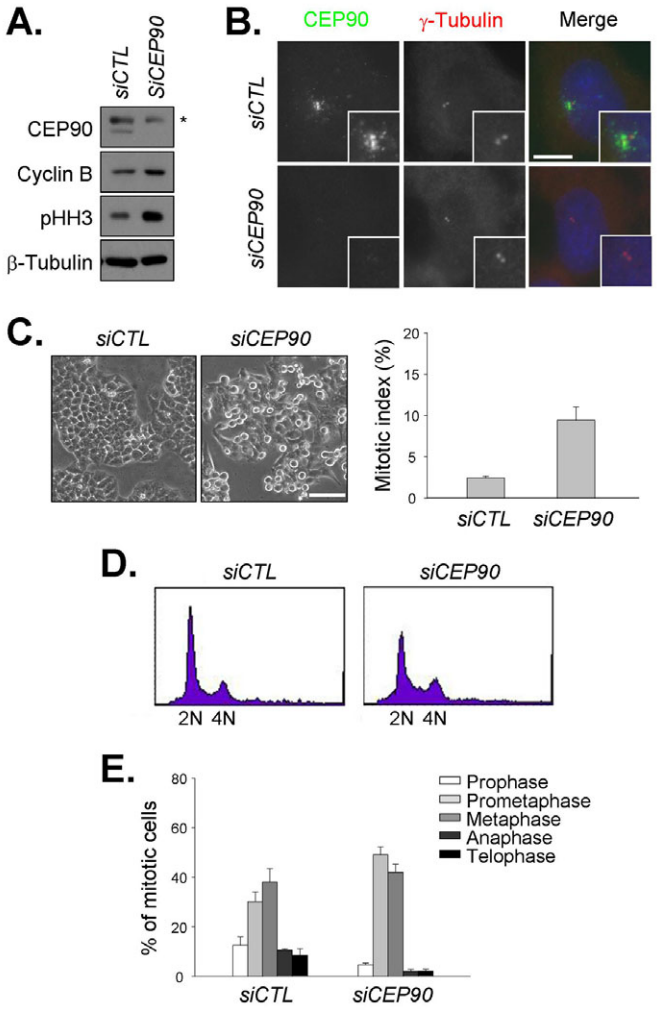

Fig. 4. Mitotic accumulation of CEP90-depleted cells. (**A**) HeLa cells were transfected with control (*siCTL*) or CEP90 (*siCEP90*) siRNA. Seventy-two hours later, the cell lysates were subjected to immunoblot analysis with antibodies specific to CEP90, cyclin B, phosphorylated histone H3 (pHH3) and β-tubulin. Asterisk indicates a nonspecific protein band. (**B**) CEP90-depleted cells coimmunostained with antibodies specific to CEP90 (green) and γ-tubulin (red). Scale bar: 10 µm. (**C**) Phase-contrast microscopic images and mitotic indices of HeLa cells transfected with *siCTL* or *siCEP90*. Scale bar: 100 µm. For statistical analysis, over 2500 cells per experimental group were analyzed in four independent experiments. The results are presented on the right as the mean ± s.e. (**D**) Cell cycle profiles determined by FACS analysis of cells transfected with *siCTL* and *siCEP90*. (**E**) Control and CEP90-depleted cells immunostained with β-tubulin antibody. DNA is stained with DAPI. Mitotic phases of the cells were determined based on the staining pattern. Cells with apparent metaphase plates were counted as metaphase cells even if they included a few misaligned chromosomes. Over 300 cells were counted in three independent experiments. Relative proportions of the mitotic phases are presented as the mean ± s.e.

CEP90 is crucial for maintaining spindle pole integrity

We next examined spindle pole defects in CEP90-depleted cells. As reported previously, most control cells had a discrete dot-like staining pattern of γ-tubulin at each spindle pole (Fig. 6A) (Khodjakov and Rieder, 1999; Lüders et al., 2006). However, the γ-tubulin signals in most of the CEP90-depleted cells appeared to be diffused along the spindle microtubules (Fig. 6A and supplementary material Fig. S1). We immunostained NuMA to recognize minus ends of the mitotic spindle microtubules (Merdes et al., 1996). NuMA was detected surrounding the γ-tubulin focus of the control spindle pole (Fig. 6B). By contrast, NuMA and γ-tubulin signals appeared mixed at spindle pole area of the CEP90-depleted cells, suggesting that the spindle poles were not organized properly (Fig. 6B). Immunostaining of the pericentrin

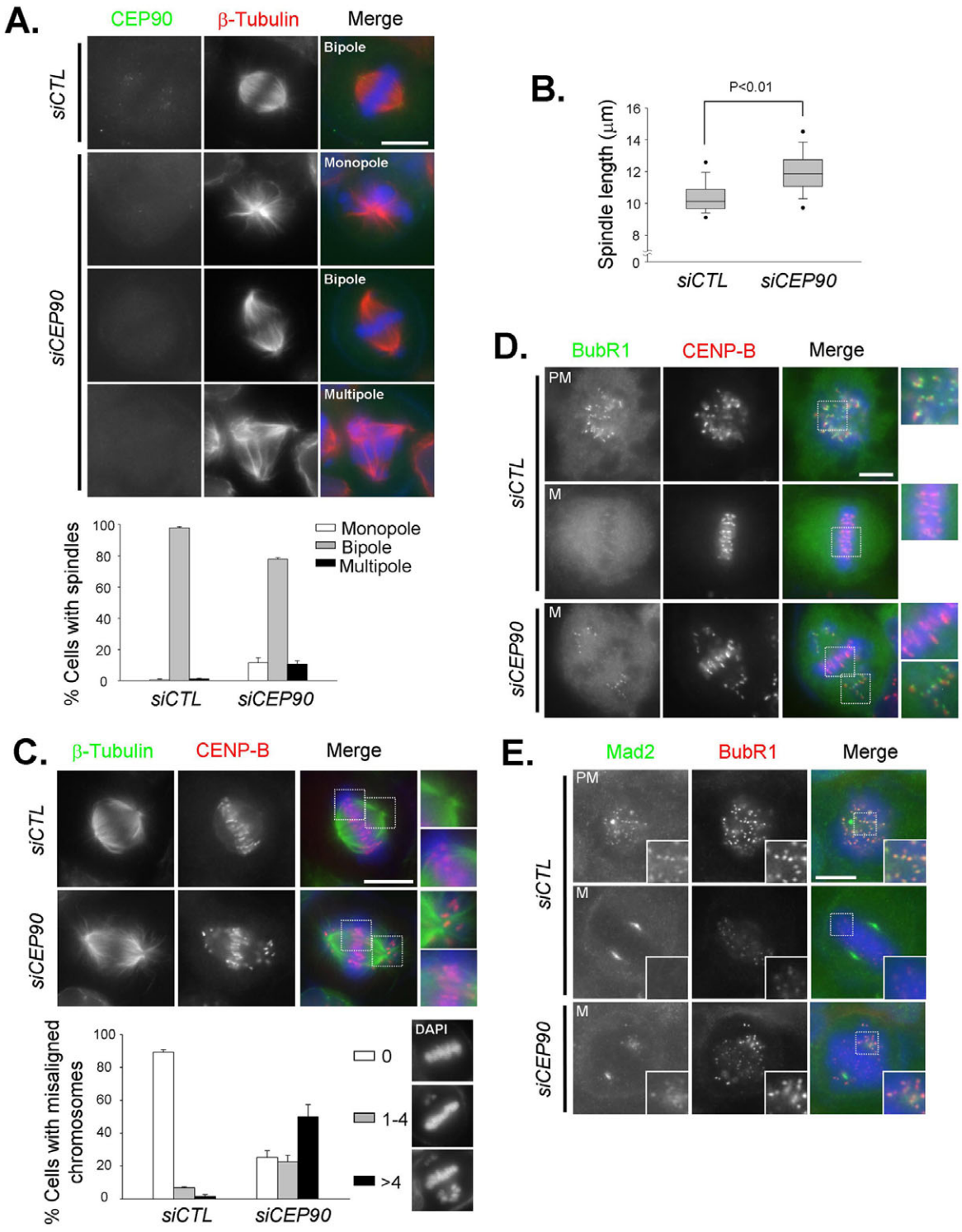

Fig. 5. Mitotic defects in CEP90-depleted cells. (**A**) HeLa cells were transfected with *siCTL* or *siCEP90*. Seventy-two hours later, the mitotic spindles were analyzed by coimmunostaining with antibodies specific to CEP90 (green) and β-tubulin (red). Scale bar: 10 μm. Over 300 spindles per experimental group were analyzed in three independent experiments. The results are presented in bottom panel as mean ± s.e. (**B**) Spindle length measured in mitotic cells with bipolar spindles. The experiments were repeated three times and 86 spindles were analyzed. The results are presented using box and whisker plots. Lines in the boxes are medians and dots outside the whiskers indicate 5th and 95th percentile outliers. *P*-value was determined using the Student's *t*-test. (**C**) HeLa cells transfected with *siCTL* or *siCEP90* coimmunostained with antibodies against β-tubulin (green) and CENP-B (red). The magnified views show the region of spindle poles (upper) and metaphase plates (lower). Scale bar: 10 μm. The number of misaligned chromosomes in the bipolar metaphase cells was counted and grouped as 0, 1–4 or >4 misaligned chromosomes (bottom). More than 300 spindles per experimental group were analyzed in three independent experiments. (**D**,**E**) HeLa cells transfected with *siCTL* or *siCEP90* coimmunostained with antibodies specific to BubR1 (green) and CENP-B (red) (D) or Mad2 (Green) and BubR1 (Red) (E). Representative prometaphase (PM) and metaphase (M) cells are shown. The magnified views show the boxed regions. Scale bar: 10 μm.

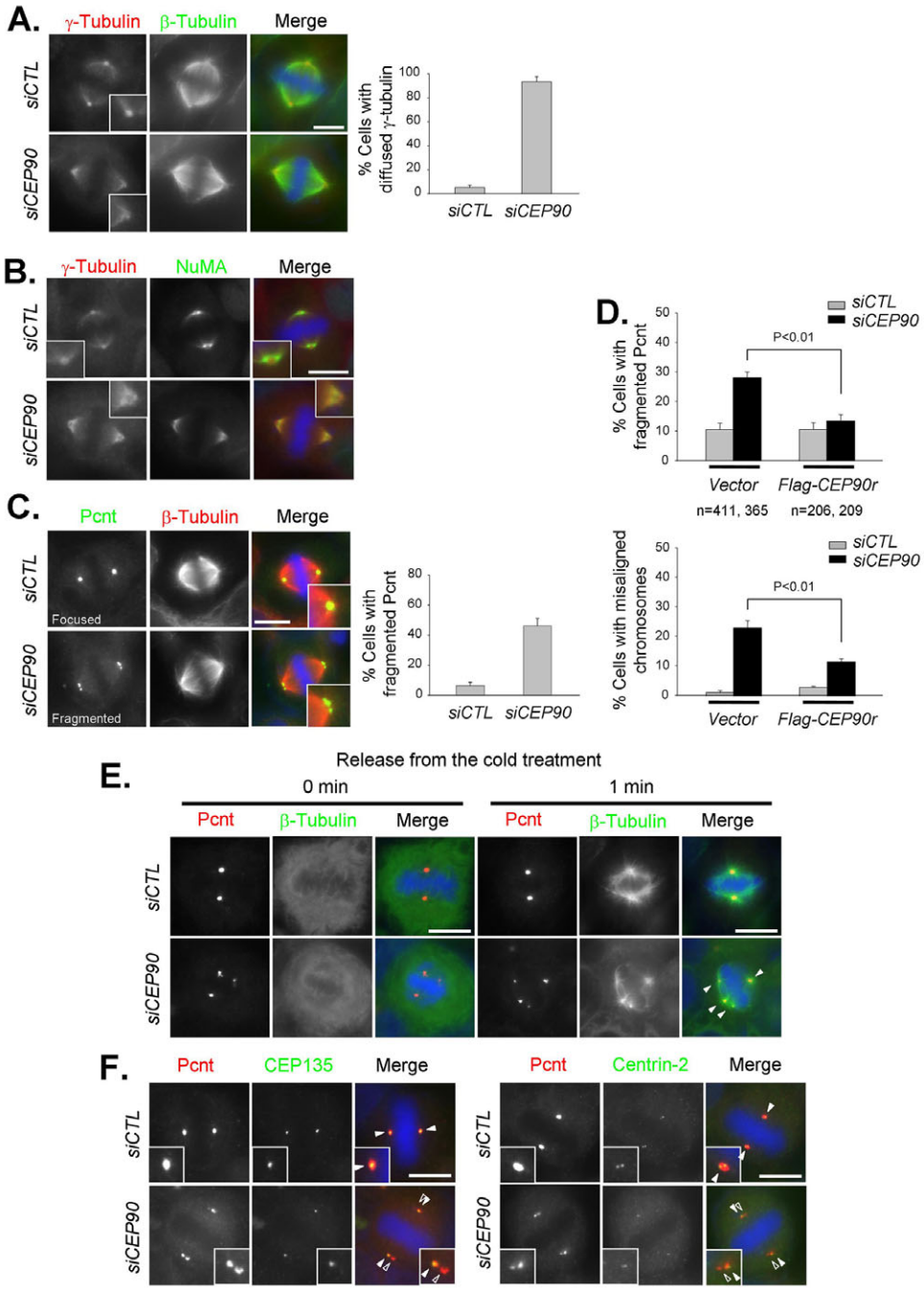

Fig. 6. CEP90 is required for spindle pole formation. (**A**) HeLa cells were transfected with *siCTL* or *siCEP90* and coimmunostained with antibodies specific to γ-tubulin (red) and β-tubulin (green). The γ-tubulin signals at spindle poles were categorized as a discrete dot or a diffuse pattern. More than 300 cells with bipolar spindles per experimental group were analyzed in three independent experiments. (**B**) *siCTL*- or *siCEP90*-transfected HeLa cells coimmunostained with antibodies specific to γ-tubulin (red) and NuMA (green). (**C**) HeLa cells were transfected with *siCTL* or *siCEP90* and coimmunostained with antibodies specific to pericentrin (Pcnt; green) and β-tubulin (red). The distribution of pericentrin was categorized as focused or fragmented. Metaphase cells with fragmented pericentrin foci were counted. For statistical analysis, more than 300 cells per experimental group were counted in three independent experiments. (**D**) HeLa cells expressing the empty vector (*Vector*) or RNAi-resistant CEP90 construct (*Flag-CEP90r*) were transfected with *siCTL* or *siCEP90*. Mitotic cells were enriched with a thymidine block and release followed by MG132 treatment during the last 90 minutes before fixation. The pericentrin (Pcnt) fragmentation and chromosome misalignment were analyzed in indicated number of metaphase cells from four independent experiments. *P*-values were determined using the Student's *t*-test. (**E**) Microtubule nucleation was induced by release from cold treatment. The cells were coimmunostained with antibodies specific to pericentrin (Pcnt; red) and β-tubulin (green). Arrowheads indicate the fragmented PCM foci from which the microtubules are nucleated. (**F**) HeLa cells were transfected with *siCTL* or *siCEP90* and coimmunostained with antibodies specific to pericentrin (Pcnt; red), along with CEP135 or centrin-2 (green). The filled and open arrowheads indicate the pericentrin foci with and without centrioles, respectively. Insets are magnified views of the spindle poles. Scale bars: 10 μm.

protein provided a clear view of the distribution of PCM. In control cells, the spindle pole looked like a discrete dot with the pericentrin antibody (Fig. 6C). However, the pericentrin signals in many of the CEP90-depleted cells appeared fragmented near the spindle poles (Fig. 6C and supplementary material Fig. S1).

To confirm that fragmented pericentrin dots and misaligned chromosomes are due to the loss of CEP90, we performed knockdown-rescue experiments. HeLa cells were infected with a lentivirus that contained the RNAi-resistant CEP90 construct (*Flag-CEP90r*). Transfection of *siCEP90* into these cells efficiently depleted endogenous CEP90 without a reduction in ectopic CEP90 levels (supplementary material Fig. S2). The RNAi-resistant CEP90 rescued the defects in centrosome integrity of CEP90-depleted cells (Fig. 6D). At the same time, the frequency of chromosome congression defects was reduced (Fig. 6D). These results confirm the involvement of CEP90 in spindle pole formation and chromosome congression.

We placed mitotic cells on ice to depolymerize spindle microtubules and observed γ-tubulin signals at the centrosomes (supplementary material Fig. S3). In CEP90-depleted cells, the centrosome-associated γ-tubulin was fragmented and colocalized with several pericentrin dots (supplementary material Fig. S3). The centrosomal pericentrin signals in CEP90-depleted mitotic cells also appeared fragmented, irrespective of cold treatment (Fig. 6E). When cells were transferred to 37°C, microtubules were nucleated from the fragmented pericentrin foci in the CEP90-depleted cells

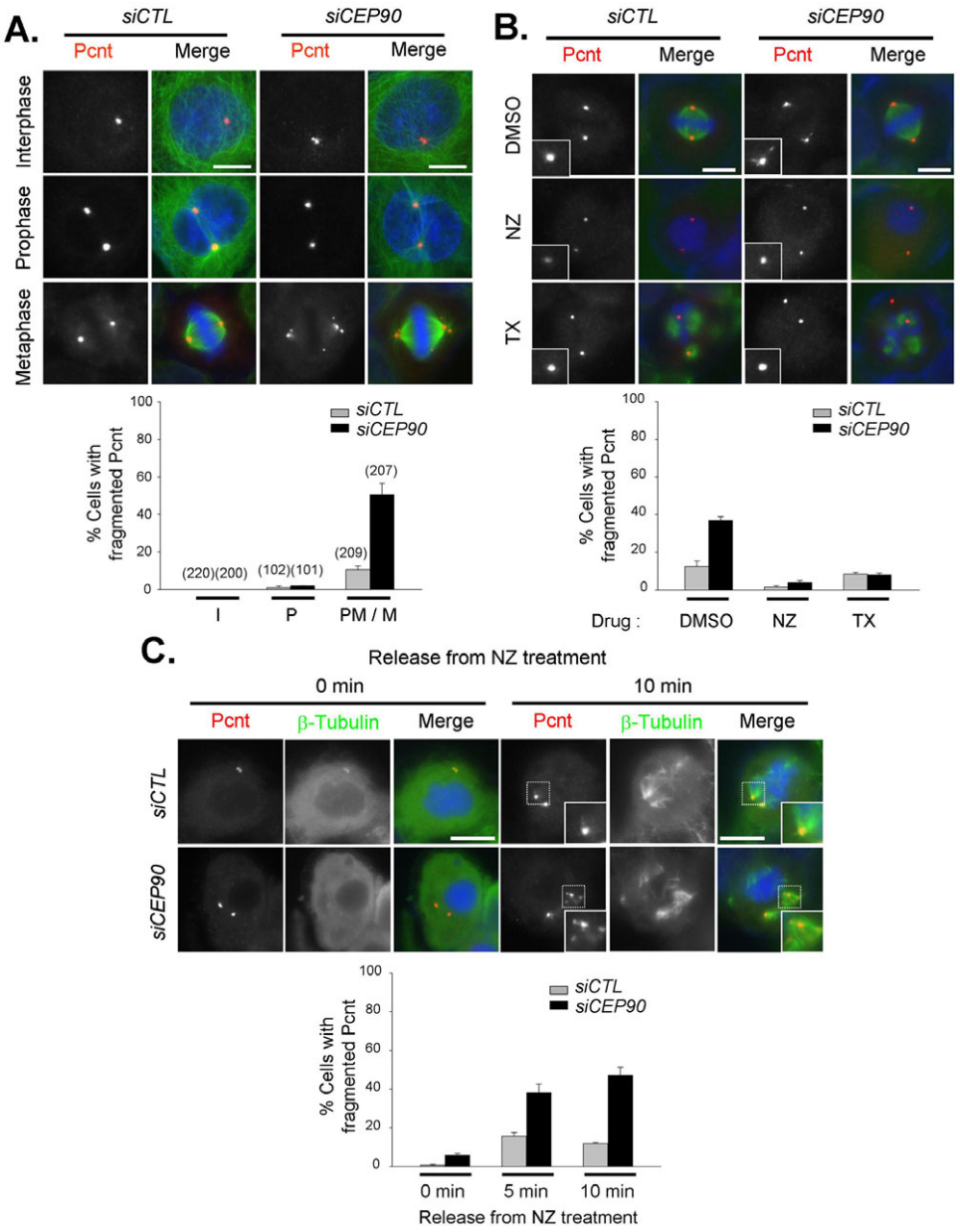

Fig. 7. Spindle pole fragmentation in CEP90-depleted cells depends on microtubule attachment at prometaphase. (**A**) HeLa cells were transfected with *siCTL* or *siCEP90* and enriched at M phase with a 9 hour release after a double thymidine block. The cells are coimmunostained with antibodies specific to pericentrin (Pcnt; red) and β-tubulin (green), and the images are merged with DAPI (Merge). The number of cells with fragmented pericentrin dots was counted. The cell cycle stages were categorized as interphase (I), prophase (P) or prometaphase–metaphase (PM/M). The number of cells per experimental group is indicated in parentheses. The experiments were repeated twice. (**B**) Cell cycle of the CEP90-depleted HeLa cells was arrested at G1–S phase with a double thymidine block and synchronously released by culturing the cells in a fresh medium. Eight hours later, when most cells were about to enter M phase, the cells were treated with nocodazole (NZ) or Taxol (TX) for 4 hours and coimmunostained with antibodies specific to pericentrin (Pcnt; red) and β-tubulin (green). The images are merged with DAPI (Merge). The control cells were treated with DMSO vehicle. The proportion of cells with fragmented pericentrin dots was counted among the prometaphase–metaphase cell population. More than 300 cells per experimental group were counted in three independent experiments. (**C**) CEP90-depleted cells were treated with nocodazole (NZ) for 3 hours and transferred to fresh medium for 0, 5 or 10 minutes. The prometaphase cells were analyzed after coimmunostaining with antibodies specific to pericentrin (Pcnt; red) and β-tubulin (green). The insets show magnified views of the centrosomes. The proportion of cells with fragmented pericentrin dots was determined at each time point. More than 300 cells per experimental group were counted in three independent experiments. Scale bars: 10 μm.

(Fig. 6E). These results revealed that the multiple centrosomes in the CEP90-depleted cells were able to nucleate microtubules and form multiple spindle poles.

To determine whether the fragmented spindle poles contained centrioles, we immunostained the cells with antibodies specific to CEP135 or centrin-2, both of which are markers for the centriole. The CEP135 and centrin-2 signals were detected in only two of several pericentrin fragments in CEP90-depleted cells (Fig. 6F). These results indicate that multiple spindle poles in CEP90-depleted mitotic cells are the result of PCM fragmentation rather than centriole amplification or splitting.

Induction of spindle pole fragmentation by the attached microtubules

We tried to pinpoint when spindle pole fragmentation occurs in CEP90-depleted cells. The centrosomes in CEP90-depleted cells looked intact until prophase of the cell cycle, but became fragmented in prometaphase and metaphase cells (Fig. 7A). To determine whether the spindle pole was fragmented by pulling and pushing forces generated by spindle microtubules and motor proteins, we treated the CEP90-depleted cells with nocodazole or Taxol around the time that cells entered mitosis (Abal et al., 2005; Oshimori et al., 2006). Both nocodazole and Taxol reduced the spindle pole fragmentation rate significantly in CEP90-depleted cells (Fig. 7B). When prometaphase cells were transferred to a drug-free medium after nocodazole treatment, microtubules started to grow from both the centrosomes and the chromosomes (Fig. 7C). At the same time, centrosome fragmentation was initiated in a time-dependent manner in the CEP90-depleted cells (Fig. 7C). This suggests that spindle pole fragmentation in CEP90-depleted cells is induced by mechanical forces of the microtubules that attach to the poles during prometaphase.

Discussion

We identified CEP90 as a component of pericentriolar satellites. CEP90 is transiently concentrated at the centrosome once cells

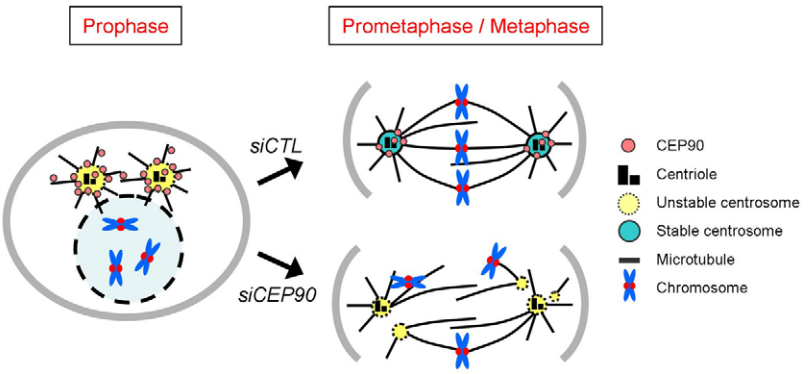

Fig. 8. A model for CEP90-dependent regulation of spindle pole integrity. CEP90 accumulates in the spindle pole once a cell enters mitosis. A robust increase in microtubule-organizing activity is observed in the spindle poles at this stage. The spindle pole should become resilient to the physical stresses derived from the pushing and pulling forces of the microtubules. The CEP90-depleted spindle poles lack structural integrity and become easily fragmented by external forces during prometaphase.

enter mitosis. Knockdown experiments revealed that CEP90 is crucial for metaphase progression during mitosis. Spindle pole fragmentation is probably the most characteristic phenotype of CEP90-depleted cells. Spindle poles were fragmented as soon as spindles attached to them, suggesting that the mechanical forces of the spindle microtubules physically stress the structure of the CEP90-depleted spindle poles. Based on these results, we propose that CEP90 is crucial for maintaining spindle pole integrity during mitosis (Fig. 8).

The multipolar spindle might be the result of spindle pole fragmentation in CEP90-depleted cells. The incidence of monopolar spindles also increased, probably as a result of abnormal accumulation of fragmented spindle poles during prometaphase progression. Despite spindle pole fragmentation, most of the CEP90-depleted cells eventually formed bipolar spindles with misaligned chromosomes near the spindle poles (Fig. 5C) (Ganem et al., 2009). The chromosomes in CEP90-depleted cells should be drawn to a spindle pole properly by astral microtubules after nuclear envelope breakdown, but might fail to be captured by microtubules from the opposite pole and eventually fail to align at the metaphase plate (Tanaka et al., 2005). The presence of BubR1- and Mad2-positive kinetochores implies defects in stable microtubule–kinetochore attachment and interkinetochore tension. Fragmented spindle poles in CEP90-depleted cells might not be able to generate enough tension. In addition, a few chromosomes might be misaligned, owing to the presence of numerous MTOCs in the CEP90-depleted cells (De Luca et al., 2008; Ganem et al., 2009). As a result, these cells with misaligned chromosomes arrest in mitosis because of spindle checkpoint (Fig. 5D,E).

It is known that the centrosome can be fragmented with unbalanced forces applied on spindle poles. The human Augmin complex HAUS localizes to interphase centrosome and to mitotic spindle microtubules and its disruption results in centrosome fragmentation and the eventual formation of multipolar spindles (Lawo et al., 2009). The HAUS complex is considered to counteract NuMA to maintain spindle pole integrity by regulating kinetochore microtubule stability and NuMA localization (Lawo et al., 2009). In fact, we also observed that NuMA localization in CEP90-depleted cells was slightly changed, but its crescent-like pattern was sustained (Fig. 6B). It remains to be examined whether CEP90 is functionally linked to the Augmin complex for spindle microtubule stability during prometaphase.

There are a few known centrosomal proteins whose depletion results in microtubule-dependent centrosome fragmentation (Cassimeris and Morabito, 2004; Oshimori et al., 2006; De Luca et al., 2008; Lawo et al., 2009). Kizuna was reported to stabilize mitotic centrosomes in a PLK1-dependent manner, presumably via physical interactions with other PCM components (Oshimori et al., 2006). Although transient accumulation of kizuna at prophase centrosomes is similar to that of CEP90, we did not find any functional link between CEP90 and kizuna. Kizuna is located at the PCM in association with the mother centriole, whereas CEP90 is mainly found at the pericentriolar satellites with a limited amount at the PCM. No physical interaction between CEP90 and kizuna was observed (data not shown). Nonetheless, we do not rule out the possibility that CEP90 is functionally related to kizuna with respect to spindle pole formation during mitosis. Recently, CEP72 was identified as a kizuna-interacting protein that is required for maintaining the centrosome integrity (Oshimori et al., 2009). CEP72 localized at pericentriole-satellite-like particles and its depletion also resulted in diffused pattern of γ-tubulin and misaligned chromosomes as well as centrosome fragmentation (Oshimori et al., 2009). It is possible that CEP90 and CEP72 are functionally linked for the spindle pole stabilization.

The exact role of CEP90 in maintaining spindle pole integrity remains to be investigated. One possibility is that CEP90 has a role in recruiting PCM scaffolds or regulators that are required for spindle pole assembly. Several centrosomal proteins are recruited to the interphase centrosome through PCM-1-dependent transport (Dammermann and Merdes, 2002; Hames et al., 2005). Transient accumulation of CEP90 and PCM-1 to the prophase centrosome might reflect an increase in centrosomal protein transport (Fig. 3) (Kubo et al., 1999; Dammermann and Merdes, 2002). It is possible that CEP90, along with PCM-1, is part of the recruiting machinery during early mitosis. In fact, the transient increase of kizuna and CEP72 at prophase centrosomes was observed (Oshimori et al., 2006; Oshimori et al., 2009). However, CEP90 and PCM-1 should make a distinct contribution to maintain spindle pole integrity, because knockdown of PCM-1 did not cause the spindle pole fragmentation (data not shown). Another possibility is that CEP90 itself is part of the PCM scaffold that maintains structural integrity against the physical forces of the attached spindles, similarly to kizuna (Oshimori et al., 2006). Even if the centrosomal levels of CEP90 fluctuate during mitosis, a substantial amount of CEP90 is detected in PCM throughout the cell cycle (Fig. 3). This centrosomal CEP90 might be crucial for prevention of the spindle pole fragmentation observed in CEP90-depleted cells.

The structure and function of pericentriolar satellites is still obscure at a molecular level. Several proteins were identified as pericentriolar satellite proteins that have interphase functions in microtubule organization or primary cilia assembly (Kim et al., 2004; Kim et al., 2008; Ge et al., 2010; Sedjaï et al., 2010). This report is the first to show that a pericentriolar satellite protein is required for mitotic progression. Our results suggest that transient

accumulation of pericentriolar satellites in early mitosis is related to spindle pole formation. In this context, additional pericentriolar satellite proteins might also be involved in mitotic events.

Materials and Methods

CEP90 cDNA and antibodies

The human *CEP90* cDNA clone (PIBF1; c13orf24, GenBank accession number: NM_006346) was purchased from the German Resource Center for Genome Research (www.rzpd.de). The cDNA was subcloned into the pGEX-4T-3 vector for purification of GST–CEP90. Anti-CEP90 rabbit polyclonal antibodies were raised against full-length CEP90 and affinity purified with GST–CEP90$^{1–757}$. Polyclonal rabbit antibodies against pericentrin, centrin-2 and BBS4 were also raised against GST–pericentrin$^{1–582}$, GST–centrin-2$^{1–172}$ and GST–BBS4$^{1–519}$, respectively. Anti-CEP135 antibody was described previously (Kim et al., 2008). Anti-PCM-1 antibody was kindly provided by Andreas Merdes (Centre National de la Recherche Scientifique/Pierre Fabre, Toulouse, France). Antibodies against phosphorylated histone H3 (Upstate), PLK1 (Zymed), Cyclin B (GNS-1, Santa Cruz Biotechnology), GAPDH (Ambion), α-tubulin (Abcam), β-tubulin (Sigma), γ-tubulin (GTU-88, Sigma; C-20, Santa Cruz Biotechnology), GFP (B-2, Santa Cruz Biotechnology), FLAG (Sigma), BubR1 (BD Transduction Laboratories), Mad2 (Covance), NuMA (Ab-2, Calbiochem) and CENP-B (H-65, Santa Cruz Biotechnology) were purchased. Alexa Fluor®555 dyes (Molecular Probes) were used for the labeling of rabbit polyclonal antibodies.

Cell culture, synchronization and drug treatment

HeLa and 293T cells were cultured in DMEM supplemented with 10% FBS at 37°C and 5% CO_2. To enrich mitotic cells, HeLa cells were synchronized at the G1–S boundary by a double thymidine block and released into fresh medium for 9 hours. To inhibit microtubule dynamics in cells entering mitosis, cells were treated with 5 μM nocodazole or 5 μM taxol 8 hours after release from the G1–S block. Microtubule depolymerization in interphase cells was performed by treating cells with 17 μM nocodazole for 2 hours.

RNAi and rescue experiments

siCEP90 (5′-GCA GCU GAC AGA GAC AUA UTT-3′), *siPCM-1* (5′-UCA GCU UCG UGA UUC UCA GTT-3′) and *siCTL* (scrambled sequence for control) (5′-GCA AUC GAA GCU CGG CUA CTT-3′) were used for RNAi experiments. The siRNAs were transfected into HeLa cells using Oligofectamine or RNAi MAX reagents (Invitrogen). For the rescue experiments, an RNAi-resistant CEP90 construct was initially introduced into HeLa cells with the lentivirus infection, and siRNAs were subsequently transfected into the cells. The RNAi-resistant CEP90 expression vector (*pFlag-CEP90r*) includes three silent mutations within the *CEP90* target sequence. The lentiviruses carrying an empty vector or *Flag-CEP90r* were produced in 293T cells using Lenti-X™ Expression system, according to manufacturer's protocol (Clontech Laboratories). HeLa cells were then incubated with the lentivirus-containing supernatant. Three to seven days after infection, the cells were transfected with *siCTL* or *siCEP90*. Mitotic cells were enriched with a thymidine block and release for 11 hours and the mitotic exit was blocked with 20 μM MG132 for the last 90 minutes before fixation.

Microtubule regrowth assay

To depolymerize microtubules, cells were incubated on ice for 60 minutes or with 1 μg/ml nocodazole for 3 hours. Microtubule regrowth was triggered by transfer to drug-free medium at 37°C.

Immunoprecipitation and immunoblotting

For immunoprecipitation, 293T cells were incubated for 30 minutes on ice with lysis buffer (50 mM Tris-HCl, pH 7.5, 150 mM NaCl, 1 mM EDTA, 50 mM NAF and 1% Triton X-100) containing protease inhibitors. The lysates were centrifuged at 12,000 r.p.m. for 20 minutes at 4°C and the supernatants were incubated with an antibody overnight, followed by incubation with protein-A–Sepharose (Amersham Pharmacia) for 2 hours at 4°C. The beads were then washed three times with the same lysis buffer and resuspended in SDS-PAGE sample buffer for immunoblot analysis, as described previously (Yoo et al., 2004).

Cell cycle profile analysis

For flow cytometry, HeLa cells were harvested by trypsinization and stained with 10 μg/ml propidium iodide. Stained cells were loaded to FACScalibur (Beckton Dickinson) and DNA contents were analyzed using Cell Quest Pro (BD Biosciences).

Immunocytochemistry, fluorescence microscopy and analyses

HeLa cells were cultured on a 12-mm coverslip and fixed with cold methanol for 10 minutes or 3.7% PFA for 15 minutes. For centrin-2 and Mad2 staining, cells were extracted with 0.1% Triton X-100 in PBS (0.1% PBST) for 30 seconds at room temperature before fixation. Fixed cells were permeabilized and blocked with 3% BSA in 0.5% PBST for 20 minutes. Antibodies were diluted in 0.1% PBST with 3% BSA. The incubation time was 1 hour for primary antibodies and 30 minutes for fluorescence-conjugated secondary antibodies. DAPI solution was used at the final step for DNA staining. Cells were mounted onto a slide glass and observed with a fluorescence microscope (Olympus IX51) equipped with a CCD camera (Qicam fast 1394, Qimaging). The images were analyzed using ImagePro 5.0 (Media Cybernetics) and statistically analyzed with SigmaPlot (Systat Software). The centrosome intensity of CEP90 was determined by first calculating the total fluorescence intensity in a fixed area of the centrosome and then subtracting the background intensity from the total intensity.

We thank A. Merdes who kindly provided us with the PCM-1 antibody. This study was supported by grants from the BioImaging Research Center at GIST, the Basic Research Program (R01-2007-000-20116-0), the SRC Program (R11-2005-009-03005-0) and the Korean Healthcare Technology R&D Project (A090558). K.K. was supported by the second stage of the Brain Korea 21 Project in 2007.

Supplementary material available online at
http://jcs.biologists.org/cgi/content/full/124/3/338/DC1

References

Abal, M., Keryer, G. and Bornens, M. (2005). Centrioles resist forces applied on centrosomes during G2/M transition. *Biol. Cell* **97**, 425-434.

Andersen, J. S., Wilkinson, C. J., Mayor, T., Mortensen, P., Nigg, E. A. and Mann, M. (2003). Proteomic characterization of the human centrosome by protein correlation profiling. *Nature* **426**, 570-574.

Cassimeris, L. and Morabito, J. (2004). TOGp, the human homolog of XMAP215/Dis1, is required for centrosome integrity, spindle pole organization, and bipolar spindle assembly. *Mol. Biol. Cell* **15**, 1580-1590.

Cho, J. H., Chang, C. J., Chen, C. Y. and Tang, T. K. (2006). Depletion of CPAP by RNAi disrupts centrosome integrity and induces multipolar spindles. *Biochem. Biophys. Res. Commun.* **339**, 742-747.

Dammermann, A. and Merdes, A. (2002). Assembly of centrosomal proteins and microtubule organization depends on PCM-1. *J. Cell Biol.* **159**, 255-266.

De Luca, M., Brunetto, L., Asteriti, I. A., Giubettini, M., Lavia, P. and Guarguaglini, G. (2008). Aurora-A and ch-TOG act in a common pathway in control of spindle pole integrity. *Oncogene* **27**, 6539-6549.

Dictenberg, J. B., Zimmerman, W., Sparks, C. A., Young, A., Vidair, C., Zheng, Y., Carrington, W., Fay, F. S. and Doxsey, S. J. (1998). Pericentrin and gamma-tubulin form a protein complex and are organized into a novel lattice at the centrosome. *J. Cell Biol.* **141**, 163-174.

Echeverri, C. J., Paschal, B. M., Vaughan, K. T. and Vallee, R. B. (1996). Molecular characterization of the 50-kD subunit of dynactin reveals function for the complex in chromosome alignment and spindle organization during mitosis. *J. Cell Biol.* **132**, 617-633.

Gaglio, T., Dionne, M. A. and Compton, D. A. (1997). Mitotic spindle poles are organized by structural and motor proteins in addition to centrosomes. *J. Cell Biol.* **138**, 1055-1066.

Ganem, N. J., Godinho, S. A. and Pellman, D. (2009). A mechanism linking extra centrosomes to chromosomal instability. *Nature* **460**, 278-282.

Garrett, S., Auer, K., Compton, D. A. and Kapoor, T. M. (2002). hTPX2 is required for normal spindle morphology and centrosome integrity during vertebrate cell division. *Curr. Biol.* **12**, 2055-2059.

Ge, X., Frank, C. L., Calderon de Anda, F. and Tsai, L. H. (2010). Hook3 interacts with PCM1 to regulate pericentriolar material assembly and the timing of neurogenesis. *Neuron* **65**, 191-203.

Gordon, M. B., Howard, L. and Compton, D. A. (2001). Chromosome movement in mitosis requires microtubule anchorage at spindle poles. *J. Cell Biol.* **152**, 425-434.

Hames, R. S., Crookes, R. E., Straatman, K. R., Merdes, A., Hayes, M. J., Faragher, A. J. and Fry, A. M. (2005). Dynamic recruitment of Nek2 kinase to the centrosome involves microtubules, PCM-1, and localized proteasomal degradation. *Mol. Biol. Cell* **16**, 1711-1724.

Khodjakov, A. and Rieder, C. L. (1999). The sudden recruitment of gamma-tubulin to the centrosome at the onset of mitosis and its dynamic exchange throughout the cell cycle, do not require microtubules. *J. Cell Biol.* **146**, 585-596.

Khodjakov, A., Copenagle, L., Gordon, M. B., Compton, D. A. and Kapoor, T. M. (2003). Minus-end capture of preformed kinetochore fibers contributes to spindle morphogenesis. *J. Cell Biol.* **160**, 671-683.

Kim, J., Krishnaswami, S. R. and Gleeson, J. G. (2008). CEP290 interacts with the centriolar satellite component PCM-1 and is required for Rab8 localization to the primary cilium. *Hum. Mol. Genet.* **17**, 3796-3805.

Kim, J. C., Badano, J. L., Sibold, S., Esmail, M. A., Hill, J., Hoskins, B. E., Leitch, C. C., Venner, K., Ansley, S. J., Ross, A. J. et al. (2004). The Bardet-Biedl protein BBS4 targets cargo to the pericentriolar region and is required for microtubule anchoring and cell cycle progression. *Nat. Genet.* **36**, 462-470.

Kim, K., Lee, S., Chang, J. and Rhee, K. (2008). A novel function of CEP135 as a platform protein of C-NAP1 for its centriolar localization. *Exp. Cell Res.* **314**, 3692-3700.

Kubo, A. and Tsukita, S. (2003). Non-membranous granular organelle consisting of PCM-1: subcellular distribution and cell-cycle-dependent assembly/disassembly. *J. Cell Sci.* **116**, 919-928.

Kubo, A., Sasaki, H., Yuba-Kubo, A., Tsukita, S. and Shiina, N. (1999). Centriolar satellites: molecular characterization, ATP-dependent movement toward centrioles and possible involvement in ciliogenesis. *J. Cell Biol.* **147**, 969-980.

Lachmann, M., Gelbmann, D., Kálmán, E., Polgár, B., Buschle, M., Von Gabain, A., Szekeres-Barthó, J. and Nagy, E. (2004). PIBF (progesterone induced blocking factor) is overexpressed in highly proliferating cells and associated with the centrosome. *Int. J. Cancer* **112**, 51-60.

Lawo, S., Bashkurov, M., Mullin, M., Ferreria, M. G., Kittler, R., Habermann, B., Tagliaferro, A., Poser, I., Hutchins, J. R., Hegemann, B. et al. (2009). HAUS, the 8-subunit human Augmin complex, regulates centrosome and spindle integrity. *Curr. Biol.* **19**, 816-826.

Lüders, J., Patel, U. K. and Stearns, T. (2006). GCP-WD is a gamma-tubulin targeting factor required for centrosomal and chromatin-mediated microtubule nucleation. *Nat. Cell Biol.* **8**, 137-147.

Mahoney, N. M., Goshima, G., Douglass, A. D. and Vale, R. D. (2006). Making microtubules and mitotic spindles in cells without functional centrosomes. *Curr. Biol.* **16**, 564-569.

Maiato, H., Rieder, C. L. and Khodjakov, A. (2004). Kinetochore-driven formation of kinetochore fibers contributes to spindle assembly during animal mitosis. *J. Cell Biol.* **167**, 831-840.

Merdes, A., Ramyar, K., Vechio, J. D. and Cleveland, D. W. (1996). A complex of NuMA and cytoplasmic dynein is essential for mitotic spindle assembly. *Cell* **87**, 447-458.

Oshimori, N., Ohsugi, M. and Yamamoto, T. (2006). The Plk1 target Kizuna stabilizes mitotic centrosomes to ensure spindle bipolarity. *Nat. Cell Biol.* **8**, 1095-1101.

Oshimori, N., Li, X., Ohsugi, M. and Yamamoto, T. (2009). Cep72 regulates the localization of key centrosomal proteins and proper bipolar spindle formation. *EMBO J.* **28**, 2066-2076.

Piehl, M., Tulu, U. S., Wadsworth, P. and Cassimeris, L. (2004). Centrosome maturation: measurement of microtubule nucleation throughout the cell cycle by using GFP-tagged EB1. *Proc. Natl. Acad. Sci. USA* **101**, 1584-1588.

Polgar, B., Kispal, G., Lachmann, M., Paar, C., Nagy, E., Csere, P., Miko, E., Szereday, L., Varga, P. and Szekeres-Bartho, J. (2003). Molecular cloning and immunologic characterization of a novel cDNA coding for progesterone-induced blocking factor. *J. Immunol.* **171**, 5956-5963.

Sedjaï, F., Acquaviva, C., Chevrier, V., Chauvin, J. P., Coppin, E., Aouane, A., Coulier, F., Tolun, A., Pierres, M., Birnbaum, D. et al. (2010). Control of ciliogenesis by FOR20, a novel centrosome and pericentriolar satellite protein. *J. Cell Sci.* **123**, 2391-2401.

Silk, A. D., Holland, A. J. and Cleveland, D. W. (2009). Requirements for NuMA in maintenance and establishment of mammalian spindle poles. *J. Cell Biol.* **184**, 677-690.

Skoufias, D. A., Andreassen, P. R., Lacroix, F. B., Wilson, L. and Margolis, R. L. (2001). Mammalian mad2 and bub1/bubR1 recognize distinct spindle-attachment and kinetochore-tension checkpoints. *Proc. Natl. Acad. Sci. USA* **98**, 4492-4497.

Szekeres-Bartho, J., Barakonyi, A., Par, G., Polgar, B., Palkovics, T. and Szereday, L. (2001). Progesterone as an immunomodulatory molecule. *Int. Immunopharmacol.* **1**, 1037-1048.

Tanaka, T. U., Stark, M. J. and Tanaka, K. (2005). Kinetochore capture and bi-orientation on the mitotic spindle. *Nat. Rev. Mol. Cell Biol.* **6**, 929-942.

Thein, K. H., Kleylein-Sohn, J., Nigg, E. A. and Gruneberg, U. (2007). Astrin is required for the maintenance of sister chromatid cohesion and centrosome integrity. *J. Cell Biol.* **178**, 345-354.

Waters, J. C., Chen, R. H., Murray, A. W. and Salmon, E. D. (1998). Localization of Mad2 to kinetochores depends on microtubule attachment, not tension. *J. Cell Biol.* **141**, 1181-1191.

Wu, G., Lin, Y. T., Wei, R., Chen, Y., Shan, Z. and Lee, W. H. (2008). Hice1, a novel microtubule-associated protein required for maintenance of spindle integrity and chromosomal stability in human cells. *Mol. Cell. Biol.* **28**, 3652-3662.

Yang, S., Liu, X., Yin, Y., Fukuda, M. N. and Zhou, J. (2008). Tastin is required for bipolar spindle assembly and centrosome integrity during mitosis. *FASEB J.* **22**, 1960-1972.

Yoo, J. C., Chang, J. R., Kim, S. H., Jang, S. K., Wolgemuth, D. J., Kim, K. and Rhee, K. (2004). NIP1/XB51/NECAB3 is a potential substrate of Nek2, suggesting specific roles of Nek2 in Golgi. *Exp. Cell Res.* **292**, 393-402.

Journal of Cell Science